PUBELESE PUBLISHER

JOAASR Journal of Advanced Applied Scientific Research

Antibacterial and anticancer properties of NiO nanoparticles by co-precipitation method

L.Umaralikhan[a*], M. Jamal Mohamed Jaffar[b],

a* Assistant Professor, Department of Physics, Jamal Mohamed College, Tiruchirappalli– 620020.

b Associate Professor& Head, Department of Physics, Jamal Mohamed College, Tiruchirappalli– 620020.

Abstract

Nickel oxide nanoparticles synthesized at room temperature (RT NiO NPs) and 60°C temperature treated nickel oxide nanoparticles (RT60 NiO NPs) were synthesized by the co-precipitation methods. The antibacterial studies performed against set of (gram positive) *S.aureus* and (gram negative) *E. coli* bacterial strains showed that the RT60 NiO NPs possessed a greater antibacterial effect as compared to the RT NiO NPs. The cytotoxic effect of the RT NiO and RT60 NiO NPs were examined in cultured (MCF-7) human breast cancer cells.

Key Words: MCF-7, Antibacterial, E. coli, S.aureus

Introduction

Nanostructure materials have attracted great interest in both fundamental as well as applied research areas due to their outstanding physical and chemical properties. High surface area metal oxides nanoparticles with the size of 1–100 nm are desirable absorbents, carriers and catalysts. The metal oxide NPs have a wide range of applications. The NiO NPs is introduced as p-type semiconductor with stable wide band gap (3.6-4.0 eV) [1], although, bulk NiO is an antiferromagnetic insulator with a Néel temperature (TN) of 523 K [2]. Important applications of nano-sized NiO include preparation of cathode materials of alkaline batteries [3], electrochemical capacitors [4], smart windows [5] and active layer for gas sensors [6]. The anticancer application, increase human and environmental exposure and thus the potential risk related to their toxicity. The Ni NPs cause cytotoxicity and apoptosis in mouse epidermal JB6 cells [7]. Ahamed *et al* have studied the oxidative stress mediated apoptosis induced by nickel ferrite NPs treated with the human lung cancer epithelial (A549) cells [8]. Mariam et al reported that Ni and NiO NPs used to study the cytotoxic effect against for human colon adenocarcinoma (HT-29) cells [9]. Kezban Adam *et al* have investigated the cytotoxicity and apoptotic effects of NiO NPs on human cervix epithelioid carcinoma (HeLa) cell line [10]. Ahamed *et al* reported that toxic response of nickel nanoparticles in human ling epithelial A546 cells [11]. Ahamed *et al* have been studied the NiO NPs exert cytotoxicity via oxidative stress and induce apoptotic response in human liver (HepG2) cancer cells [12]. Duan *et al* reported that the NiO NPs induce apoptosis through repressing SIRT1 in human bronchial epithelial cancer cells [13]. Ramasami *et al* investigated antimicrobial activity was tested against the two bacterial (*B. cereus* and *K. aerogenes*) strains and one fungal (*C. albicas*) treated with NiO NPs [14]. Talebian *et al* studied antibacterialactivity was tested against two common foodborne pathogenic bacteria *S. aurous* and *E.coli* used to test for NiO NPs [15]. Various methods are available for the synthesis of metal oxide nanoparticles, such as a chemical method [16], physical method [17] and green method [18, 19]. In the present investigation, NiO NPs are synthesized by the co-precipitation method. We have studied the structural, antibacterial and anticancer properties of the NiO NPs.

Experimental methods

Synthesis of RT NiO and RT60 NiO was carried out using analytical grade Nickel nitrate hexahydrate [$Ni(NO_3)_2$. $6H_2O$]and sodium hydroxide (NaOH) were used as the precursors without further purification.

Synthesis process of RT NiO, the amount of Nickel nitrate (0.1M) was completely dissolved in deionized water and a required amount of aqueous NaOH (0.8M) solution was added drop wise to the aqueous Nickel nitrate solution. The solution was stirred 5h and maintained at room temperature. Later, a green colour precipitate was formed slowly. The green colour precipitate was washed several times with double distilled water and ethanol. The precipitate was dried at 120°C. Thus, NiO nano-powder was obtained. The schematic diagram for the preparation of the NiO NPs samples is shown in Fig. 1.

Similarly synthesis processor of RT60 NiO, the amount of Nickel nitrate (0.1M) was completely dissolved in deionized water and a required amount of aqueous NaOH (0.8M) solution was added drop wise to the aqueous Nickel nitrate solution. The solution was stirred 5h and maintained at 60°C temperature. Later, a green colour precipitate was formed slowly. The green colour precipitate was washed several times with double distilled water and ethanol. The precipitate was dried at 120°C. Thus, NiO nano-powder was obtained. The obtained NiO samples were annealed at 700°C in air for 5 h. Finally, NiO nanoparticles was collected and used for further studies.

Antimicrobial activity of NiO NPs

Antimicrobial activity of the RT NiO and RT60 NiO NPs were done by agar well diffusion method against two pathogenic bacterial strains *S.aureus* (gram positive) and *E. coli* (gram negative) on Muller-Hinton agar, according to the Clinical and Laboratory Standards Institute (CLSI) [20]. The media plates (MHA) were streaked with bacteria 2-3 times by rotating the plate at 60◦ angles for each streak to ensure the homogeneous distribution of the inoculums. Then the agar plates were swabbed with 100 mL each of overnight cultures of *S.aureus* and *E.coli* using a sterile L-shaped glass rod. Using a sterile cork-borer, wells (6 mm) were created in each petri plate. Varied concentrations of NiO NPs (1mg/ml, 3mg/ml and 5mg/ml for both G+ and G- both bacteria) were loaded onto the petri plates followed by incubation for 24 h at 37°C, for bacteria. After the incubation period, the diameter of the zone of inhibition (DZI) was recorded. Kanamycin (Hi-Media) was used as the positive control against gram negative and gram positive bacteria respectively to compare the efficacy of the test samples.

Anticancer activity

Cell culture

The MCF-7 breast adenocarcinoma cancer cells were cultured in RPMI 1640 medium (Sigma-Aldrich, St. Louis, MO, USA), supplemented with 10% fetal bovine serum (Sigma, USA) and 10,000 IU penicillin and 100 μg/ml of streptomycin as antibiotics (Himedia, Mumbai, India), in 96 well culture plates, at 37°C, in a humidified atmosphere of 5% CO_2, in a CO_2 incubator (Forma, Thermo Scientific, USA). All experiments were performed using cells from passage 15 or less.

MTT assay

The of the RT NiO and RT60 NiO NPs were suspended in dimethyl sulfoxide (DMSO), diluted in culture medium and used to treat the chosen cell line (MCF-7) over a complex concentration range of 5-100μg/ml for 24 h . DMSO solution was used as the solvent control. A miniaturized viability assay using 3-(4, 5-di-methylthiazol-2-yl)-2, 5-diphenyl-2H-tetrazolium bromide (MTT) was carried out (Mosmann *et al*; 1983[21]). To each well, 20 μl of 5 mg/ml MTT in phosphate buffer (PBS) was added. The plates were wrapped with aluminum foil and incubated for 4 h at 37°C. The purple formazan product was dissolved by the addition of 100 μL of 100% DMSO to each well. The absorbance was monitored at 570 nm (measurement) and 630 nm (reference) using a 96 well plate reader (Biorad 680). The data were collected for four replicates. The percentage of inhibition was calculated from this data using the formula

$$\frac{\text{mean OD of untreated cells (control)} - \text{mean OD of treated cells}}{\text{mean OD of untreated cells (control)}} \times 100$$

Acridine Orange (AO) and Ethidium bromide (EB) staining

AO/EB staining was performed as described by Spector *et al*. The cell suspension of each sample containing 30,000 cells/mL cells, was treated with 200 μLof AO/EB solution (100 μL/mg AO and 100 μL/mg EB in PBS) and examined by a Olympus inverted fluorescence microscope (Ti-Eclipse) using a UV filter (450-490 nm). One hundred cells per sample were counted in tetraplicate for each dose point. The cells were scored as viable, apoptotic or necrotic as judged by the fluorescence emittance, nuclear morphology and membrane integrity [22]. The morphological changes were also observed and photographed.

Chaterization techniques

The NiO NPs were characterized by X-ray diffractometer (model: X'PERT PRO PANalytical). The diffraction pattern was recorded in the range of 25º-80º for the NiO NPs samples where the monochromatic wavelength of 1.54 Å used. The morphology of the synthesized NiO NPs was examined using HRTEM. Sample for HRTEM analysis was prepared by drop coating the nanoparticles solutions on carbon-coated copper grids at room temperature. The excess nanoparticles solutions

were removed with filter paper. The copper grid was finally dried at room temperature and was subjected to TEM analysis by the instrument Tecnai F20 model operated at an accelerating voltage of 200 kV. The samples were analyzed by EDAX (model: ULTRA 55). The FT-IR spectrum was recorded in the range of 400-4000 cm^{-1} by using Perkin-Elmer spectrometer.

Results and discussion

The antibacterial activities have been reported against (gram positive) *S.aureus* and (gram negative) *E. coli* bacterial pathogens were used for three different concentrations of RT NiO and RT60 NiO NPs samples (1 mg/ml, 3mg/ml and 5 mg/ml) as shown in Fig. 1(a-d). Table 1 shows the size of the zone of inhibition for both NiO NPs loaded with test samples. The samples containing 1mg/ ml of NiO NPs, RT NiO (6mm and 6mm) and RT60 NiO NPs (size of 13 mm and 12 mm for both bacterial strain) at lowest concentration did not excepts any zone of inhibition. Further increasing the concentration of both NiO NPs (3 mg/ml and 5 mg/ ml), whereas Zone of inhibition rate also increases (Table-1) for *S. aureus* and *E. coli* respectively. However, the RT60 NiO NPs shows the highest antibacterial activity as compared to RT NiO NPs.The antibacterial efficiency of NiO NPs generally depends on the presence of more ROS, which is mainly attributed to the smaller particles size and less agglomerated particles, diffusion ability of the reactant molecules [23], increasing the lattice constant [24], the release of Ni^{2+}, morphology etc., Moreover, electrostatic attraction between negatively charged bacterial cells and positively charged nanoparticles is crucial for the activity of nanoparticles as bactericidal materials. This interaction not only inhibits the bacterial growth but also induces the Reactive Oxygen Species (ROS) generation, which leads to cell death [25, 26]. The oxide nanoparticles are interaction with the bacterial cell walls and possible permeation of the nanoparticulated oxide into the bacterial cells [27]. The proposed that the induction of intracellular oxidative stress is to be a key event of the toxicity mechanisms of the metal-oxide nanoparticles. The oxide nanoparticles enter inside the cell, this nanomaterial may induce intracellular oxidative stress by disturbing the balance between oxidant and anti-oxidant processes. From the oxidative stress induced by exposure to nanomaterials may stimulate an increase of the cytosolic calcium concentration or may cause the translocation of transcription factors to the nucleus, which regulate pro-inflammatory genes. Alternatively, exceeding oxidative stress may also modify proteins, lipids and nucleic acids, which further stimulates the anti-oxidant defense system or even leads to cell death [28].

The photo-catalysis seems to be the most important anti-microbial mechanism; reactive oxygen species (ROS) produced on the surface of these NPs in the presence of light cause oxidative stress in microbial cell and eventually leads to the death of the cell. ROS contain the most reactive hydroxyl radical ($^{\bullet}OH$), less toxic superoxide anion radical ($^{\bullet}O_2^-$) and hydrogen peroxide with a weaker oxidizer (H_2O_2). The generation of H_2O_2 can penetrate into the cell membrane and kill the microbes [29]. The mechanism of light induced generation of ROS can be given as follows [30].

$$NiO + h\upsilon \rightarrow e^- + h^+$$
$$h^+ + H_2O \rightarrow {}^{\bullet}OH + H^+$$
$$e^- + O_2 \rightarrow {}^{\bullet}O_2^-$$
$$^{\bullet}O_2^- + H^+ \rightarrow HO_2^{\bullet}$$
$$HO_2^{\bullet} + H^+ \rightarrow H_2O_2$$

As mentioned earlier, the greater number of ROS is mainly attributed to the smaller particles size and less agglomerated particles, diffusion ability of the reactant molecules, increasing the lattice constant. The interactions of ZnO nanoparticles with the bacterial cell membranes and the generation of damage on bacterial surface have been suggested as responsible for the antibacterial activity. Kasemets *et al* have been report the antibacterial activity of ZnO, CuO and TiO_2 results from the direct contact of

nanoparticles with bacterial membrane [31].The high surface area has a beneficial effect on the activity for catalysts. Therefore, the crystallite size may play a critical role in the biocide activity. Zhang *et al* reported that smaller crystal size with a higher surface area leads to higher antibacterial activity [32].From the XRD patterns, the crystallite size of RT NiO and RT60 NiO NPs are found to be 43 nm and 34nm respectively.

Yamamoto *et al* reported that the antibacterial efficiency of the nanoparticles generally depends on the presence of more ROS, which is mainly attributed to the lattice constant [33]. In our result, the lattice constant values are 4.1806 Å and 4.1874 Å for RT NiO and RT60 NiO NPs respectively. The RT60 NiO NPs had the highest values of lattice constant as compared to the RT60 NiO NPs, causing to the generation of more hydrogen peroxide (H_2O_2) [24]. In the case of biotic systems exposed to the nanoparticles, H_2O_2 immediately oxidizes the biomolecules, releasing electrons. In abiotic conditions, the H_2O_2 reacts with Fe^{4+} (oxidation by gaining an electron), producing stable Fe^{3+} in the trap levels within the nanoparticles [25].

The less agglomerated particles also one of the reason for greater number of ROS. From the HRTEM image how that decrease agglomerated particles RT60 NiO NPs as compare to the RT NiO NPs.Other way, the possible mechanisms are involving the interaction of nanomaterials with the biological macromolecules.

Cytotoxicity studies

The cytotoxic effect of the RT NiO and RT60 NiO NPs is examined on cultured MCF- 7 human breast cancer cells by exposing cells for 24 h to medium containing the NiO NPs at 5-100µg/ml concentration (Table 2). In our results, that there is direct dose-response relationship with tested cells at higher concentrations. In relation to cell death, a minimum of 65 and 55µg/ml for RT NiO and RT60 NiO NPs are well enough to induce 50% of cell mortality, RT60 NiO NPs was well enough to induce 50% cell mortality as compared RT NiO NPs. The RT60NiO NPs showed the highly effective cytotoxic activity against MCF-7 cancer cells.

The microorganisms carry a negative charge while metal oxides carry a positive charge [33]. This creates an "electromagnetic" attraction between the microbe and treated surface. The Metal oxide NPs contact with microbes, the microbe oxidizes and dies instantly.

Haja hameed *et al* reported that the antibacterial activity is that when the Zn^{2+} released by ZnO comes into contact with the cell membranes of the microbe, the cell membranes with negative charge and Zn^{2+} with positive charge mutually attract Zn^{2+} penetrates into the cell membrane and react with sulfhydryl groups inside the cell membrane. As a result, the activity of synthetize in the microbe becomes so damaged that the cellulose the ability of growth through cell division, which leads to the death of the microbe [34]. In our result XRD and HRTEM shows the decrease the particles size for RT60 NiO NPs as compare to the RT NiO NPs, decrease particles size increase the Ni^{2+} ion release. The more Ni^{2+} ions release come in to contact with cell membrane, this Ni^{2+} ions higher damage to bacteria cell membrane and bind with DNA replication, cell division and thereby the surface area of bacterial cell membrane is increased. These intracellular functional changes establish the oxidative stress induced by ROS generation due to the cell expiry. Figure 1 shows the schematic diagram of antimicrobial mechanism. The RT60 NiO NPs as compare to the RT NiO NPs as more antibacterial efficiency due to the temperature effect as per the above results.

The nanoparticles can lead to the spontaneous ROS generation at their surface owing to their chemical and surface characteristics, including the generation of free radical (superoxide anion ($^{\cdot}O_2^-$), hydroxyl radical ($OH^{\cdot}$), hydrogen

peroxide (H_2O_2) and singlet oxygen ($^1O_2$)). ROS are generated intrinsically or extrinsically within the cell, after their interaction with cellular components, e.g., mitochondrial damage. The molecular oxygen generates $\cdot O_2$, which is the primary ROS via one electron reduction catalyzed by nicotinamide adenine dinucleotide phosphate (NADPH) oxidase. Further reduction of oxygen may either lead to H_2O_2 or $OH^{\cdot}$ via dismutation and metal-catalyzed Fenton reaction respectively [35,36] and another way, the nanoparticles owing to their small size are capable of reaching the nucleus and interact with DNA [37-39]. They may also exhibit an indirect effect on DNA through their ability to generate ROS [39]. This DNA damage may either lead to carcinogenesis or cell death, thus disrupting normal cell functions.

As mentioned earlier, the greater number of ROS is mainly attributed to the smaller particles size and less agglomerated particles, diffusion ability of the reactant molecules, increasing the lattice constant (detail are explain in antibacterial section).The reactive oxygen species (ROS), such as superoxide anions and hydrogen peroxide (H_2O_2) are normal byproducts of cellular aerobic metabolism and superoxide anions ($\cdot O_2^-$) are secondarily converted to (H_2O_2) by the superoxide dismutase (SOD). H_2O_2 has a dual role in cellular homeostasis and low level of intracellular H_2O_2 stimulated cell growth [40], whereas high levels of H_2O_2 lead to cellular senescence and apoptosis [41]. Conduction electrons and valence holes in semiconductors such as metal oxide have been traditionally used for photocatalytic oxidation of organic and inorganic pollutants, and as sensitizers for photo-destruction of cancer cells [42, 43] via oxidative damage and the electrons and holes were typically produced via UV irradiation and excitation. When NPs are synthesized by using specialized methods, more numbers of holes and/or electrons might be available even without the presence of UV light. The holes are powerful oxidants and they can react with water or surface-bound chemisorbed hydroxyl groups to produce hydroxyl radicals. The conduction band electrons are good reductants, and can move to the particle surface and be trapped in metastable surface states, or react with electron acceptors or oxidants such as adsorbed O_2. Various activated oxygen species can be produced by the reactions of holes and electrons in a metal oxide semiconductor impact indicate that ROS play crucial role in eukaryotic cell death by NiO NPs. The NiO NPs induced cytotoxicity in MCF-7 cells. Cells were exposed to different concentrations (5-100 μg/ml) of NiO NPs for 24 h. At the end of exposure cell viability was determined as described in the materials and methods for MTT assays. Data represented are mean ± SD of three identical experiments made in three replicate.*Significant difference as compared to the controls ($p < 0.05$ for each).

Fluorescent Staining Method

The characteristic morphological changes absorbed RT NiO and RT60 NiO NPs are treated on MCF-7 human breast cancer cells. This MCF-7 cells are evaluated by adopting fluorescent microscopic analysis of Acridine orange/EthBr (AO/EB) stained cells (see Fig. 3). The RT NiO and RT60 NiO NPs induce cell death through different modes like apoptosis and necrosis. The cells were treated with IC_{50} concentration and apoptosis is a gene-controlled cell death process, which is characterized by DNA fragmentation, chromatin condensation and marginalization, membrane blebbing, cell shrinkage, and fragmentation of cells into membrane-enclosed vesicles or apoptotic bodies to be phago-cytosed by macrophages [44].

The cytological changes were classified into four types according to the fluorescence emission and morphological features of chromatin condensation in the AO/EB-stained nuclei:(i) viable cells having uniformly green fluorescing nuclei with highly organized structure; (ii) early apoptotic cells having green fluorescing nuclei but with perinuclear chromatin condensation visible as bright-green patches or fragments; (iii)

late apoptotic cells having orange-to-red fluorescing nuclei with condensed or fragmented chromatin; (iv) necrotic cells, swollen to large sizes, having uniformly orange-to-red fluorescing nuclei with no indication of chromatin fragmentation. These morphological changes are indicating that the cells are committed to death. The RT60 NiO NPs possesses the higher of apoptosis morphology as compared to the RT60 NiO NPs as shown in Fig. 3(a-c).

Conclusions

In summary, the NiO NPs were synthesized by co-precipitation method. The antibacterial studies performed against a *S. auras* and *E. coli* bacterial strains showed that the RT60 NiO NPs possessed a greater antibacterial effect than the RT NiO NPs. The cytotoxic effect of the NiO NPs was examined on cultured MCF-7 human breast cancer cells by exposing cells for 24 h. Among them, the RT60 NiO NPs showed the highest anticancer activity. Relating to cell death, a minimum concentration of 55 μg/ml of RT60 NiO NPs was well enough to induce less than 50% of cell mortality as compared RT NiO NPs.

References

[1] Yang, H., Tao, Q., Zhang, X., Tang, A., & Ouyang, J. (2008). Solid-state synthesis and electrochemical property of SnO 2/NiO nanomaterials. Journal of Alloys and Compounds, 459(1), 98-102.

[2] Díaz-Guerra, C., Remon, A., Garcia, J. A., & Piqueras, J. (1997). Cathodoluminescence and photoluminescence spectroscopy of NiO. physica status solidi (a), 163(2), 497-503.

[3] Bahadur, J., Sen, D., Mazumder, S., & Ramanathan, S. (2008). Effect of heat treatment on pore structure in nano-crystalline NiO: A small angle neutron scattering study. Journal of Solid State Chemistry, 181(5), 1227-1235.

[4] Nathan, T., Aziz, A., Noor, A. F., & Prabaharan, S. R. S. (2008). Nanostructured NiO for electrochemical capacitors: synthesis and electrochemical properties. Journal of Solid State Electrochemistry, 12(7-8), 1003-1009.

[5] Granqvist, C. G. (Ed.). (1995). Handbook of inorganic electrochromic materials. Elsevier.

[6] Hotovy, I., Huran, J., Spiess, L., Hascik, S., & Rehacek, V. (1999). Preparation of nickel oxide thin films for gas sensors applications. Sensors and Actuators B: Chemical, 57(1), 147-152.

[7] Zhao, J., Bowman, L., Zhang, X., Shi, X., Jiang, B., Castranova, V., & Ding, M. (2009). Metallic nickel nano-and fine particles induce JB6 cell apoptosis through a caspase-8/AIF mediated cytochrome c-independent pathway. Journal of nanobiotechnology, 7(1), 2.

[8]Ahamed, M., Akhtar, M. J., Siddiqui, M. A., Ahmad, J., Musarrat, J., Al-Khedhairy, A. A., & Alrokayan, S. A. (2011). Oxidative stress mediated apoptosis induced by nickel ferrite nanoparticles in cultured A549 cells. Toxicology, 283(2), 101-108.

[9] Mariam, A. A., Kashif, M., Arokiyaraj, S., Bououdina, M., Sankaracharyulu, M. G. V., Jayachandran, M., & Hashim, U. (2014). BIO-SYNTHESIS OF NiO AND Ni NANOPARTICLES AND THEIR CHARACTERIZATION. DIGEST JOURNAL OF NANOMATERIALS AND BIOSTRUCTURES, 9(3), 1007-1019.

[10] Ada, K., Turk, M., Oguztuzun, S., Kilic, M., Demirel, M., Tandogan, N., & Latif, O. (2010). Cytotoxicity and apoptotic effects of nickel oxide nanoparticles in cultured HeLa cells. Folia Histochemica et Cytobiologica, 48(4), 524-529.

[11] Ahamed, M. (2011). Toxic response of nickel nanoparticles in human lung epithelial A549 cells. Toxicology in Vitro, 25(4), 930-936.

[12] Ahamed, M., Ali, D., Alhadlaq, H. A., & Akhtar, M. J. (2013). Nickel oxide nanoparticles exert cytotoxicity via oxidative stress and induce apoptotic response in human liver cells (HepG2). Chemosphere, 93(10), 2514-2522.

[13] Duan, W. X., He, M. D., Mao, L., Qian, F. H., Li, Y. M., Pi, H. F., & Zhang, L. (2015). NiO nanoparticles induce apoptosis through repressing SIRT1 in human bronchial epithelial

cells. Toxicology and applied pharmacology, 286(2), 80-91.
[14] Ramasami, A. K., Reddy, M. V., & Balakrishna, G. R. (2015). Combustion synthesis and characterization of NiO nanoparticles. Materials Science in Semiconductor Processing, 40, 194-202.
[15] Talebian, N., Doudi, M., & Kheiri, M. (2014). The anti-adherence and bactericidal activity of sol–gel derived nickel oxide nanostructure films: solvent effect. Journal of sol-gel science and technology, 69(1), 172-182.
[16] Devi, P. G., & Velu, A. S. (2015). Synthesis by co-precipitation method, structural and optical properties of ZnO and nickel doped ZnO nanoparticles. JOURNAL OF ADVANCED APPLIED SCIENTIFIC RESEARCH, 1(2), 130-137.
[17] Ma, C. L., & Sun, X. D. (2002). Preparation of nanocrystalline metal oxide powders with the surfactant-mediated method. Inorganic Chemistry Communications, 5(10), 751-755.
[18] Umaralikhan, L., & Jaffar, M. J. M. Green Synthesis of MgO Nanoparticles and it Antibacterial Activity. Iranian Journal of Science and Technology, Transactions A: Science, 1-9.
[19] Ali, M. R., Umaralikhan, L., & Jaffar, M. (2015). Antibacterial Effect of Silver Nanoparticles Synthesized Using Curcuma Aromatica Leaf Extract.
[20] Wright, G. D. (2000). Resisting resistance: new chemical strategies for battling superbugs. Chemistry & biology, 7(6), R127-R132.
[21] Mosmann, T. (1983). Rapid colorimetric assay for cellular growth and survival: application to proliferation and cytotoxicity assays. Journal of immunological methods, 65(1-2), 55-63.
[22] Spector, P. (1998). Cells a Laboratory Manual Vol3: Subcellular Localization of Genes and Their Products.
[23] Noble, M. A. (2005). Bacteria in Biology, Biotechnology and Medicine, Paul Singleton. West Sussex, England: John Wiley & Sons Ltd., 2004, 570 pp., ISBN 0-470-09027-8. *Clinical Chemistry*, *51*(12), 2428-2428.
[24] Yamamoto, O., Komatsu, M., Sawai, J., & Nakagawa, Z. E. (2004). Effect of lattice constant of zinc oxide on antibacterial characteristics. *Journal of materials science: materials in medicine*, *15*(8), 847-851.
[25] Xia, T., Kovochich, M., Brant, J., Hotze, M., Sempf, J., Oberley, T., & Nel, A. E. (2006). Comparison of the abilities of ambient and manufactured nanoparticles to induce cellular toxicity according to an oxidative stress paradigm. *Nano letters*, *6*(8), 1794-1807.
[26] Xia, T., Kovochich, M., Liong, M., Mädler, L., Gilbert, B., Shi, H., & Nel, A. E. (2008). Comparison of the mechanism of toxicity of zinc oxide and cerium oxide nanoparticles based on dissolution and oxidative stress properties. *ACS nano*, *2*(10), 2121-2134.
[27] Jiang, W., Mashayekhi, H., & Xing, B. (2009). Bacterial toxicity comparison between nano-and micro-scaled oxide particles. *Environmental pollution*, *157*(5), 1619-1625.
[28] Karunakaran, C., Gomathisankar, P., & Manikandan, G. (2010). Preparation and characterization of antimicrobial Ce-doped ZnO nanoparticles for photocatalytic detoxification of cyanide. *Materials Chemistry and Physics*, *123*(2), 585-594.
[29] Fang, M., Chen, J. H., Xu, X. L., Yang, P. H., & Hildebrand, H. F. (2006). Antibacterial activities of inorganic agents on six bacteria associated with oral infections by two susceptibility tests. *International Journal of Antimicrobial Agents*, *27*(6), 513-517.
[30] Dutta, R. K., Nenavathu, B. P., Gangishetty, M. K., & Reddy, A. V. R. (2012). Studies on antibacterial activity of ZnO nanoparticles by ROS induced lipid peroxidation. *Colloids and Surfaces B: Biointerfaces*, *94*, 143-150.
[31]. Kasemets, K., Ivask, A., Dubourguier, H. C., & Kahru, A. (2009). Toxicity of nanoparticles of ZnO, CuO and TiO 2 to yeast Saccharomyces cerevisiae. *Toxicology in vitro*, *23*(6), 1116-1122.
[32] Zhang, L., Ding, Y., Povey, M., & York, D. (2008). ZnO nanofluids–A potential antibacterial

agent. *Progress in Natural Science*, *18*(8), 939-944.
[33] Hosseinkhani, P., Zand, A. M., Imani, S., Rezayi, M., & Rezaei Zarchi, S. (2011). Determining the antibacterial effect of ZnO nanoparticle against the pathogenic bacterium, Shigella dysenteriae (type 1). *International Journal of Nano Dimension*, *1*(4), 279-285.
[34] Hameed, A. S. H., Karthikeyan, C., Sasikumar, S., Kumar, V. S., Kumaresan, S., & Ravi, G. (2013). Impact of alkaline metal ions Mg 2+, Ca 2+, Sr 2+ and Ba 2+ on the structural, optical, thermal and antibacterial properties of ZnO nanoparticles prepared by the co-precipitation method. *Journal of Materials Chemistry B*, *1*(43), 5950-5962.
[35] Vallyathan, V., & Shi, X. (1997). The role of oxygen free radicals in occupational and environmental lung diseases. *Environmental Health Perspectives*, *105*(Suppl 1), 165.
[36] Thannickal, V. J., & Fanburg, B. L. (2000). Reactive oxygen species in cell signaling. *American Journal of Physiology-Lung Cellular and Molecular Physiology*, *279*(6), L1005-L1028.
[37] Chen, M., & von Mikecz, A. (2005). Formation of nucleoplasmic protein aggregates impairs nuclear function in response to SiO 2 nanoparticles. *Experimental cell research*, *305*(1), 51-62.
[38] Sharma, V., Singh, S. K., Anderson, D., Tobin, D. J., & Dhawan, A. (2011). Zinc oxide nanoparticle induced genotoxicity in primary human epidermal keratinocytes. *Journal of nanoscience and nanotechnology*, *11*(5), 3782-3788.
[39] Shukla, R. K., Sharma, V., Pandey, A. K., Singh, S., Sultana, S., & Dhawan, A. (2011). ROS-mediated genotoxicity induced by titanium dioxide nanoparticles in human epidermal cells. *Toxicology in Vitro*, *25*(1), 231-241.
[40] Sundaresan, M., Yu, Z. X., Ferrans, V. J., Irani, K., & Finkel, T. (1995). Requirement for generation of H2O2 for platelet-derived growth factor signal transduction. *Science*, *270*(5234), 296-299.
[41] Bernard, D., Gosselin, K., Monte, D., Vercamer, C., Bouali, F., Pourtier, A., & Abbadie, C. (2004). Involvement of Rel/nuclear factor-κB transcription factors in keratinocyte senescence. *Cancer research*, *64*(2), 472-481.
[42] Cai, R.; Hashimoto, K.; Itoh, K.; Kubota, Y.; Fujishima, A., Photokilling of malignant cells with ultrafine TiO2 powder. Bull. Chem. Soc. Jpn., 1991, 64(4), 1268-1273.
[43] Kubota, Y., Shuin, T., Kawasaki, C., Hosaka, M., Kitamura, H., Cai, R., & Fujishima, A. (1994). Photokilling of T-24 human bladder cancer cells with titanium dioxide. *British journal of cancer*, *70*(6), 1107.
[44] Møller, P., Knudsen, L. E., Loft, S., & Wallin, H. (2000). The comet assay as a rapid test in biomonitoring occupational exposure to DNA-damaging agents and effect of confounding factors. *Cancer Epidemiology Biomarkers & Prevention*, *9*(10), 1005-1015.

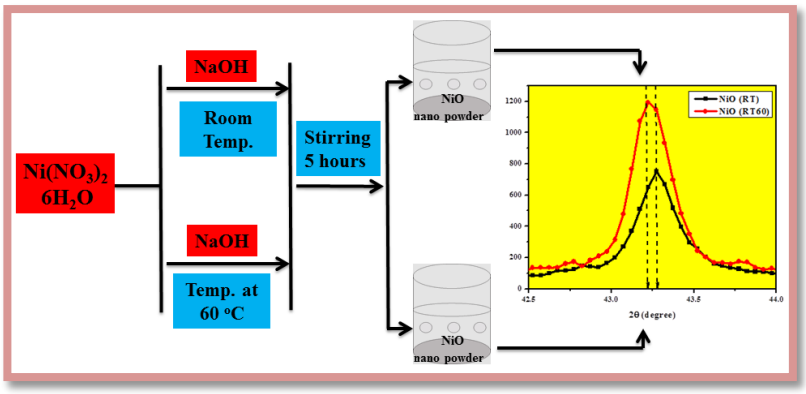

Figure 1 Schematic diagram for the formation of NiONPs.

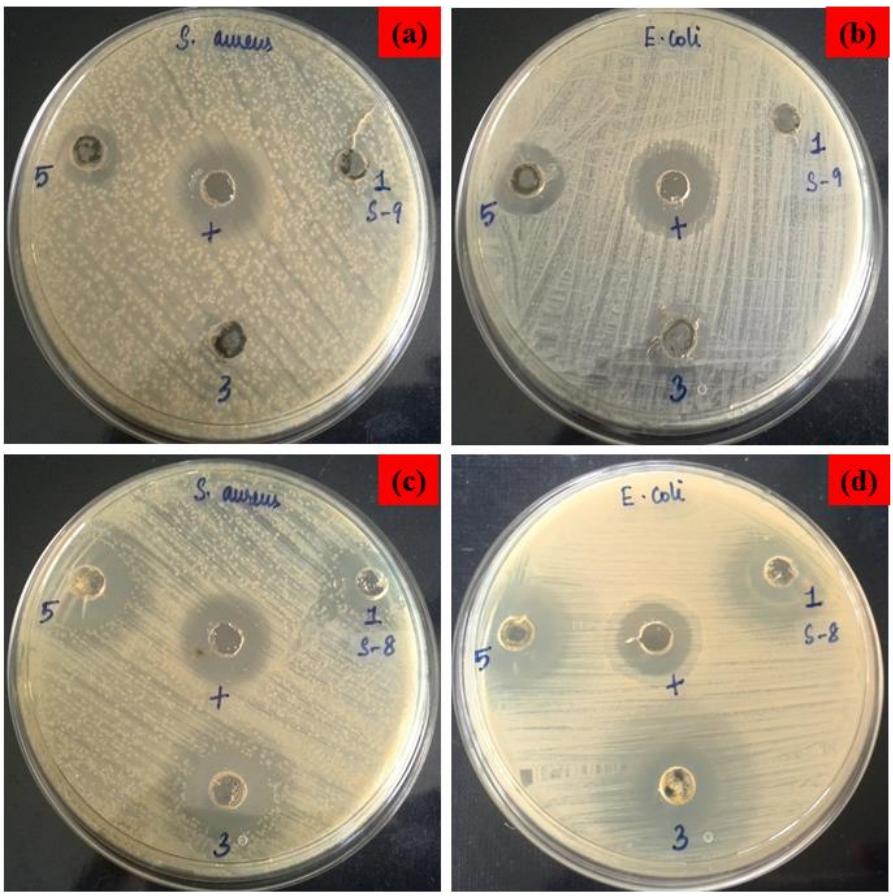

Figure 1 Size of the zone of inhibition formed around each well, loaded with test samples, indicating the antibacterial activity of (a) RT NiO (*S. aureus*), (b) RT NiO (*E. Coli*), (c) RT60 NiO (*S. aureus*) and (d) RT60 NiO (*E. Coli*) for G+ and G− bacterial strains.

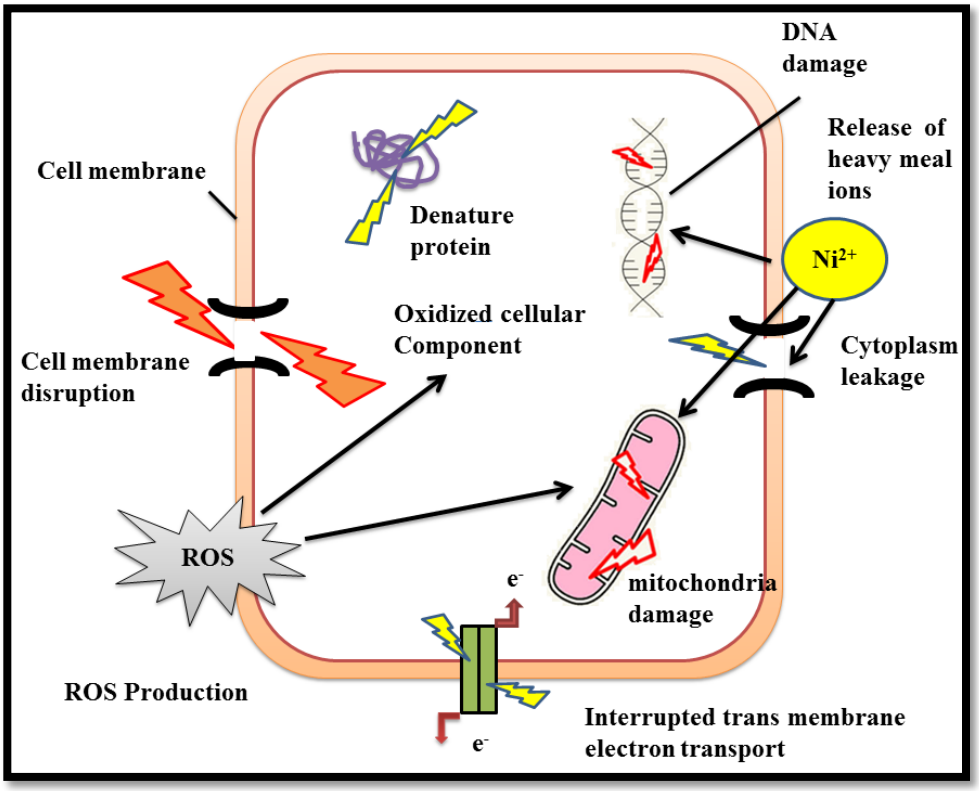

Figure 2 Diagrammatic representation of toxicity of NiO NPs against bacterial pathogens

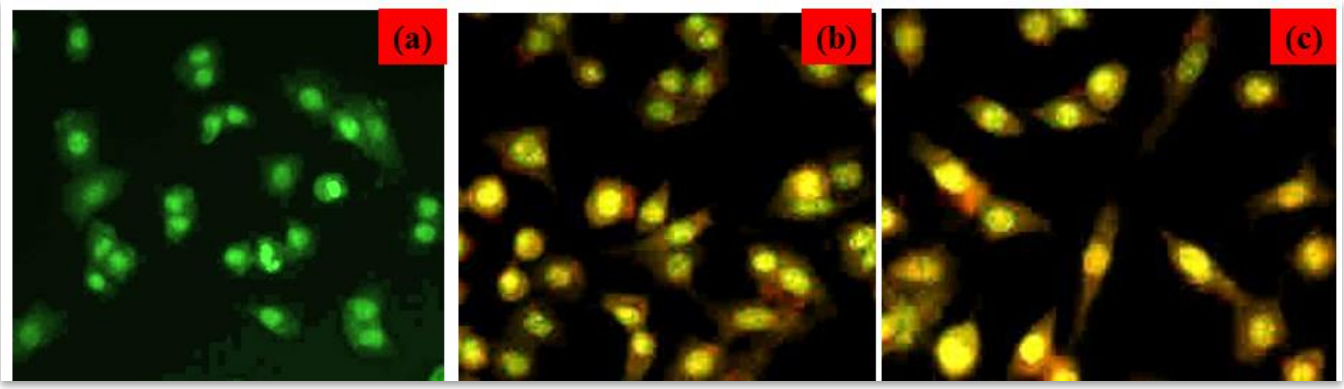

Figure 3(a-c) Cells were treated NiO with IC_{50} concentrations and the morphological changes were observed using a fluorescent microscope after staining with AO/EB for (a) control, (b) RT NiO NPs and (c) RT60 NiO NPs.

Sample	Control	1mg/ml	3mg/ml	5mg/ml
RT NiO (*S. aureus*)	14	6	7	11
RT NiO (*E. Coli*)	15	6	12	14
RT60 NiO (*S. aureus*)	18	13	15	18
RT60 NiO (*E. Coli*)	15	12	15	16

Table 1 Zone of inhibition for NiO NPs against G+ and G−bacterial strains

Concentrations (μg/ml) *	RT NiO NPs	RT60 NiO NPs
Control	100	100
5	93.3233	97.4
15	88.69	90.46
25	80.57	77.558
35	69.4667	62.5096
45	61.61	59.4153
55	57.5467	49.57
65	50.3067	44.65
75	40.2474	39.4167
85	35.4467	33.996
100	26.6453	24.419

Table 2 The effect of NiO NPs reduced cell viability of human breast cancer cell line (MCF-7).